Article

Complexed Nitrogen Heterosuperbenzene: The Coordinating Properties of a Remarkable Ligand

Sylvia M. Draper, Daniel J. Gregg, Emma R. Schofield, Wesley R. Browne, Marco Duati, Johannes G. Vos, and Paolo Passaniti

J. Am. Chem. Soc., **2004**, 126 (28), 8694-8701• DOI: 10.1021/ja0491634 • Publication Date (Web): 22 June 2004

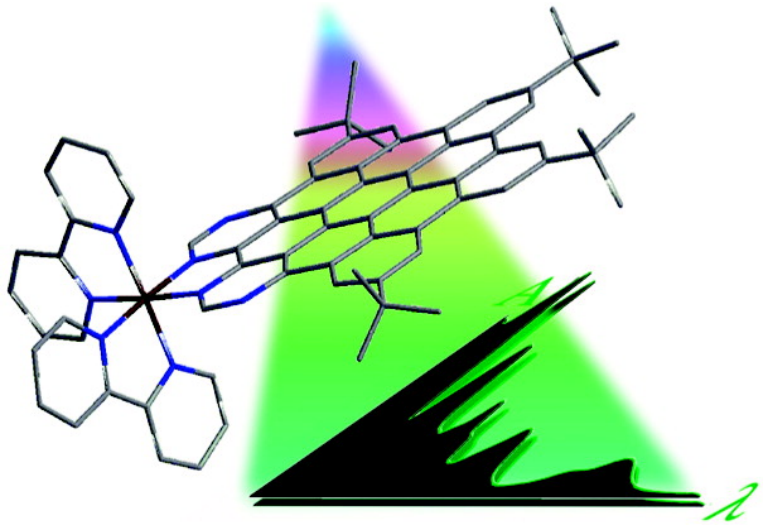

J|A|C|S
ARTICLES
Published on Web 06/22/2004

Complexed Nitrogen Heterosuperbenzene: The Coordinating Properties of a Remarkable Ligand

Sylvia M. Draper,*,† Daniel J. Gregg,† Emma R. Schofield,† Wesley R. Browne,‡ Marco Duati,‡ Johannes G. Vos,‡ and Paolo Passaniti§

Contribution from the Department of Chemistry, University of Dublin, Trinity College, D2, Ireland, The National Centre for Sensor Research, School of Chemical Science, Dublin City University, D9, Ireland, and Dipartimento di Chimica "G. Ciamician", Università di Bologna, 40126 Bologna, Italy

Received February 16, 2004; E-mail: smdraper@tcd.ie

Abstract: Tetra-*peri*-(*tert*-butyl-benzo)-di-*peri*-(pyrimidino)-coronene **1**, the parent compound of the nitrogen heterosuperbenzene family N−HSB, is employed as a novel monotopic ligand in the formation of [Pd(η^3-C_3H_5)(**1**)]PF_6 **2** and [Ru(bpy)$_2$(**1**)]$(PF_6)_2$ (where bpy = 2,2′-bipyridine **3a** and d_8-2,2′-bipyridine **3b**). These N-coordinated complexes are fully characterized by ^{1}H NMR and IR spectroscopy and ESI-MS. Metal coordination has a profound effect on both the absorption and the emission properties of **1**. Pd(II) coordination causes a red-shift in the low-energy absorptions, a decrease in the intensity of the n−π* absorptions, and a quenching of the emission. Ru(II) coordination causes absorption throughout the visible region and creates two new complexes that join an elite group of compounds known as "black" absorbers. **3a** and **3b** possess two discernible ^{1}MLCT bands. The one of exceptionally low energy (λ_{max} = 615 nm) has an associated ^{3}MLCT emission (λ_{max} = 880 nm) due to the unprecedented electron delocalization and acceptor properties of the rigid aromatic N−HSB **1**. Both Ru(II) complexes are near-IR emitters with unusually protracted emission lifetimes of 320 ns at 77 K. They are photochemically inert, and their electrochemical properties are consistent with the presence of a low-lying π* orbital on **1**. The first two reversible reductions ($E_{1/2}$ (CH_3CN), −0.54 V, −1.01 V vs SCE) are due to the stepwise reduction of **1** and are anodically shifted as compared to $[Ru(bpy)_3]^{2+}$. Temperature- and concentration-dependent NMR studies on **2** and **3a** suggest extensive aggregation is occurring in solution.

Introduction

In recently published work, we introduced tetra-*peri*-(*tert*-butyl-benzo)-di-*peri*-(pyrimidino)-coronene **1** as the first member of an electronically and structurally unique class of compounds, the nitrogen heterosuperbenzenes, N−HSBs.[1] As with Mullen's hexabenzocoronenes,[2] these fused polyaromatics exhibit an extraordinary degree of delocalization. However, the inclusion of nitrogen donor atoms renders the hexabenzocoronene-type cores overall electron-accepting and confers on the new N−HSBs the dual advantages of ligand functionality and increased solubility. Such unusual characteristics offer the opportunity to study supramolecular effects such as π-stacking and to probe the electronic behavior of the N−HSBs as ligands. The self-assembly of molecules is critical in the context of supramolecular chemistry and in the design of nanodevices.[2b,3] The presence of 13 fused aromatic rings in **1** would be expected to confer aggregation properties to it and its complexes.

In the present contribution, the investigation of the coordinating abilities of **1**, the founding member of the N−HSB family, is explored through the influence of this fascinating ligand on the physical and spectroscopic properties of transition-metal centers. Complexes of Pd(II) with similarly bulky ligands are being developed for catalysis,[4] while complexes of both Pd(II) and Ru(II) with rigid, delocalized aromatic ligands have unusual electronic properties.[5,6] The wavelength of both the lowest-energy ^{1}MLCT (metal-to-ligand charge transfer) absorption and ^{3}MLCT-based luminescence bands of conjugated Ru(II) polypyridyl complexes are typically shifted to lower energy. This

† University of Dublin.
‡ Dublin City University.
§ Università di Bologna.

(1) Draper, S. M.; Gregg, D. J.; Madathil, R. *J. Am. Chem. Soc*. **2002**, *124*, 3486−3487.
(2) (a) Watson, M. D.; Fechtenkötter, A.; Müllen, K. *Chem. Rev.* **2001**, *101*, 1267−1300. (b) Herwig, P. T.; Kayser, C. W.; Müllen, K.; Spiess, H. W. *Adv. Mater*. **1996**, *8*, 510−513. (c) Stabel, A.; Herwig, P. T.; Müllen, K.; Rabe, J. *Angew. Chem., Int. Ed. Engl.* **1995**, *34*, 1609−1611. (d) van de Craats, A. M.; Warman, J. M.; Fechtenkötter, A.; Brand, J. D.; Harbison, M.; Müllen, K. *Adv. Mater.* **1999**, *11*, 1469−1472.
(3) Scheibel, T.; Parthasarathy, R.; Sawicki, G.; Lin, X.-M.; Jaeger, H.; Lindquist, S. L. *Proc. Natl. Acad. Sci. U.S.A.* **2003**, *100*, 4527−4532.
(4) Dijkstra, H. P.; Steenwinkel, P.; Grove, D. M.; Lutz, M.; Spek, A. L.; van Koten, G. *Angew. Chem., Int. Ed.* **1999**, *38*, 2185−2188.
(5) (a) Balzani, V.; Juris, A.; Venturi, M.; Campagna, S.; Serroni, S. *Chem. Rev.* **1996**, *96*, 759−833. (b) Balzani, V.; Scandola, F. *Supramolecular Photochemistry*; Ellis Horwood: Chichester, UK, 1991. (c) Meyer, T. J. *Pure Appl. Chem.* **1986**, *58*, 1193−1206. (d) Meyer, T. J. *Pure Appl. Chem.* **1990**, *62*, 1003−1009. (e) Juris, A.; Balzani, V.; Barigelletti, F.; Campagna, S.; Belser, P.; von Zelewsky, A. *Coord. Chem. Rev.* **1988**, *84*, 85−277. (f) De Cola, L.; Belser, P. *Coord. Chem. Rev.* **1998**, *177*, 301−346. (g) Treadway, J. A.; Strouse, G. F.; Ruminski, R. R.; Meyer, T. J. *Inorg. Chem.* **2001**, *40*, 4508−4509. (h) Aiello, I.; Ghedini, M.; La Deda, M. *J. Lumin.* **2002**, *96*, 249−259.
(6) Albano, G.; Belser, P.; De Cola, L.; Gandolfi, M. T. *Chem. Commun*. **1999**, 1171−1172.

10.1021/ja0491634 CCC: $27.50

provides access to Ru(II)-based black MLCT absorbers and near-IR emitters.[5g,7,8] To date, a limited range of large-surface ligands have been used in Ru(II) coordination chemistry.[9] However, there is interest in the application of large-surface, bridging ligands such as eilatin (a tetraaza heptacyclic aromatic alkaloid), for the purpose of investigating long-range electron- and energy-transfer processes.[5a,f,10]

To explore the versatility of our potentially bidentate ligand, we focused the current investigation on late transition-metal centers that typically adopt square-planar (Pd(II)) and octahedral (Ru(II)) geometries. For the former, $[Pd(allyl)]^+$ is employed as the reactive metal fragment, generating a compound containing a potentially active catalytic center bound to a bulky, carbon-rich graphite-like sheet.[11] For the latter, the $Ru(bpy)_2$-fragment[5] was the obvious choice to demonstrate how the electron-accepting nature of our new diimine ligand **1** would transform the photophysical properties of a heteroleptic complex. In addition, the d_8-bpy analogue was prepared to investigate the nature of the Ru(II)-based emission, as deuteriation has been shown to increase bpy-based emission lifetimes dramatically.[12] To illustrate the features described, Pd(II) complex **2** and Ru(II) complexes **3a**, **3b**, and **5** (Scheme 1) have been synthesized and spectroscopically characterized.

Results and Discussion

Synthesis and Characterization of 2. The cationic (η^3-allyl)-Pd(II) complex **2** was prepared from $[Pd(\eta^3\text{-}C_3H_5)(CH_3CN)_2](NO_3)$ formed in situ from the dimer $[Pd(\eta^3\text{-}C_3H_5)(\mu\text{-}Cl)]_2$[13] (Scheme 1). The dark red complex was characterized as its PF_6^- salt by ^{1}H NMR, IR spectroscopy, ESI-mass spectrometric, and accurate mass analyses. Elemental analysis of **2** could not be obtained, due to incomplete combustion, an artifact of the extremely high thermal stability of the aromatic core of **1**.[14]

Confirmation of the bidentate nature of the coordination was obtained by comparing the ^{1}H NMR spectrum of **2** in $CDCl_3$ with that of the free ligand. The atom-labeling scheme is shown in Scheme 1. The five singlets in the aromatic region correspond to the five N−HSB **1** proton environments H1−H5, which is consistent with the C_{2v} symmetry of complex **2**. Downfield shifts were observed for the aromatic protons

Scheme 1. N−HSB Ligand **1** and the Synthetic Route for Generating $[Pd(\eta^3\text{-}C_3H_5)(\mathbf{1})]^+$ **2**, $[Ru(bpy)_2(\mathbf{1})]^{2+}$ **3a**, $[Ru(d_8\text{-}bpy)_2(\mathbf{1})]^{2+}$ **3b**, and $[Ru(bpy)_2(\mathbf{4})]^{2+}$ **5**[a]

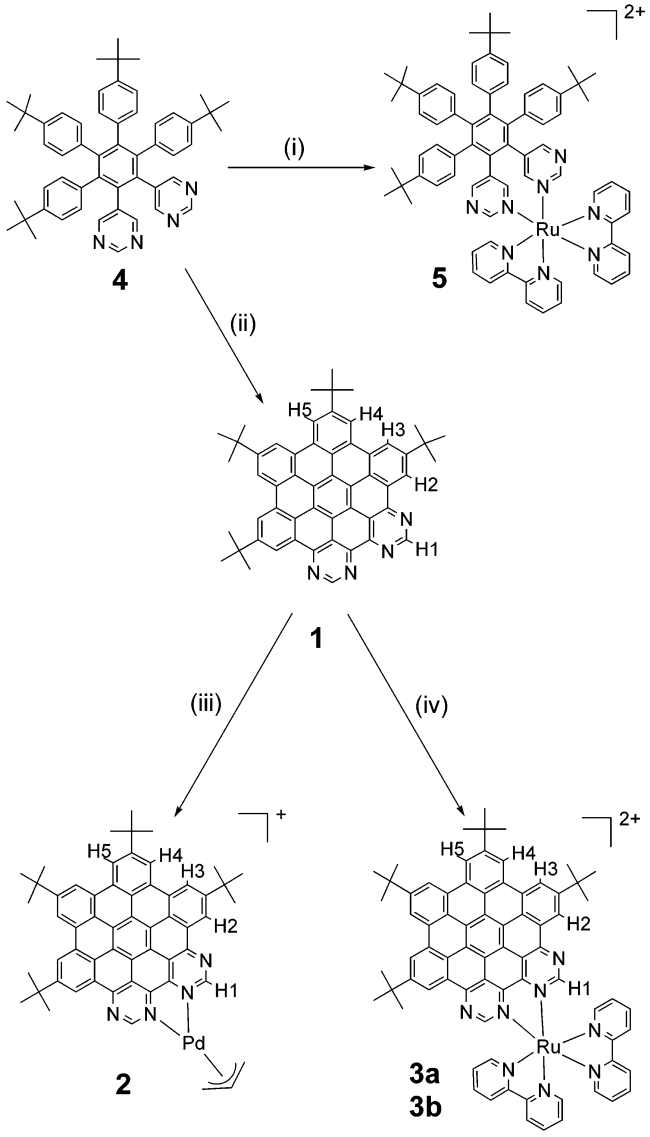

[a] Reaction conditions: (i) $[Ru(bpy)_2(CH_3COCH_3)_2]^{2+}$, argon, 391 K, 72 h, *n*-butanol; (ii) ref 1; (iii) $[Pd(\eta^3\text{-}C_3H_5)(CH_3CN)_2](NO_3)$, argon, room temperature, 12 h, toluene/acetonitrile; (iv) $[Ru(bpy)_2Cl_2]$ or $[Ru(d_8\text{-}bpy)_2Cl_2]$, argon, 400 K, 20 h, diethylene glycol ethyl ether.

H2−H5, from δ 8.9−9.4 in the free ligand to δ 9.2−9.45 in **2**. However, the proton signal assigned to H1 shifted upfield (δ 9.79 to δ 8.56) as a result of its proximity to the shielding allyl group. The allyl signals appear as broad singlets at δ 5.61 (meso proton), δ 4.24 (syn protons), and δ 2.87 (anti protons), while the four *tert*-butyl groups are present in the aliphatic region as two singlets, each integrating for 18 protons. The ^{1}H NMR signals for the allyl and N−HSB protons of **2** sharpen and exhibit a downfield shift on increasing temperature which we attribute to aggregation effects (vide infra).[15]

Electronic Absorption and Emission Properties of 2. To probe the absorption and emission properties of both N−HSB **1** and its (η^3-allyl)Pd(II) complex **2**, the free ligand was titrated with $[Pd(\eta^3\text{-}C_3H_5)(CH_3CN)_2](NO_3)$, and the spectral changes were recorded (see Figure 1). Coordination has a profound effect

(7) (a) Chiorboli, C.; Bignozzi, C. A.; Scandola, F.; Ishow, E.; Gourdon, A.; Launay, J.-P. *Inorg. Chem.* **1999**, *38*, 2402−2410. (b) Nazeeruddin, M. K.; Péchy, P.; Grätzel, M. *Chem. Commun.* **1997**, 1705−1706.
(8) Anderson, P. A.; Strouse, G. F.; Treadway, J. A.; Keene, F. R.; Meyer, T. J. *Inorg. Chem.* **1994**, *33*, 3863−3864 and references within.
(9) Glazer, E. C.; Tor, Y. *Angew. Chem., Int. Ed.* **2002**, 41, 4022−4026.
(10) (a) Gourdon, A.; Launay, J.-P. *Inorg. Chem.* **1998**, *37*, 5336−5341. (b) Ishow, E.; Gourdon, A.; Launay, J.-P.; Chiorboli, C.; Scandola, F. *Inorg. Chem.* **1999**, *38*, 1504−1510. (c) Gut, D.; Goldberg, I.; Kol, M. *Inorg. Chem.* **2003**, *42*, 3483−3491.
(11) (a) Tsuji, J. *Palladium Reagents and Catalysts, Innovation in Organic Synthesis*; Wiley: Chichester, 1995. (b) Tsuji, J.; Takahashi, H.; Morikawa, M. *Tetrahedron Lett.* **1965**, *49*, 4387−4388. (c) Trost, B. M.; Verhoeven, T. R. *J. Am. Chem. Soc.* **1976**, *98*, 630−632. (d) Trost, B. M.; Van Vranken, D. L. *Chem. Rev.* **1996**, *96*, 395−422. (e) Canal, J. M.; Gómez, M.; Jiménez, F.; Cano, F. H. *Organometallics* **2000**, *19*, 966−978. (f) Canovese, L.; Visentin, F.; Chessa, G.; Niero, A.; Uguagliati, P. *Inorg. Chim. Acta* **1999**, *293*, 44−52. (g) Jikei, M.; Ishida, Y.; Kakimoto, M.; Imai, Y. *React. Funct. Polym.* **1996**, *30*, 117−124. (h) Satake, A.; Koshino, H.; Nakata, T. *Organometallics* **1999**, *18*, 5108−5111. (i) Tsukada, N.; Sato, T.; Mori, H.; Sugawara, S.; Kabuto, C.; Miyano, S.; Inoue, Y. *J. Organomet. Chem.* **2001**, *627*, 121−126.
(12) Browne, W. R.; Coates, C. G.; Brady, C.; Matousek, P.; Towrie, M.; Botchway, S. W.; Parker, A. W.; Vos, J. G.; McGarvey, J. J. *J. Am. Chem. Soc.* **2003**, *125*, 1706−1707.
(13) Sakakibara, M.; Takahashi, Y.; Sakai, S.; Ishii, Y. *J. Chem. Soc., Chem. Commun.* **1969**, 396−397.
(14) Simpson, C. D.; Brand, J. D.; Berresheim, A. J.; Przybilla, L.; Räder, H. J.; Müllen, K. *Chem.-Eur. J.* **2002**, *8*, 1424−1429.

(15) See Supporting Information.

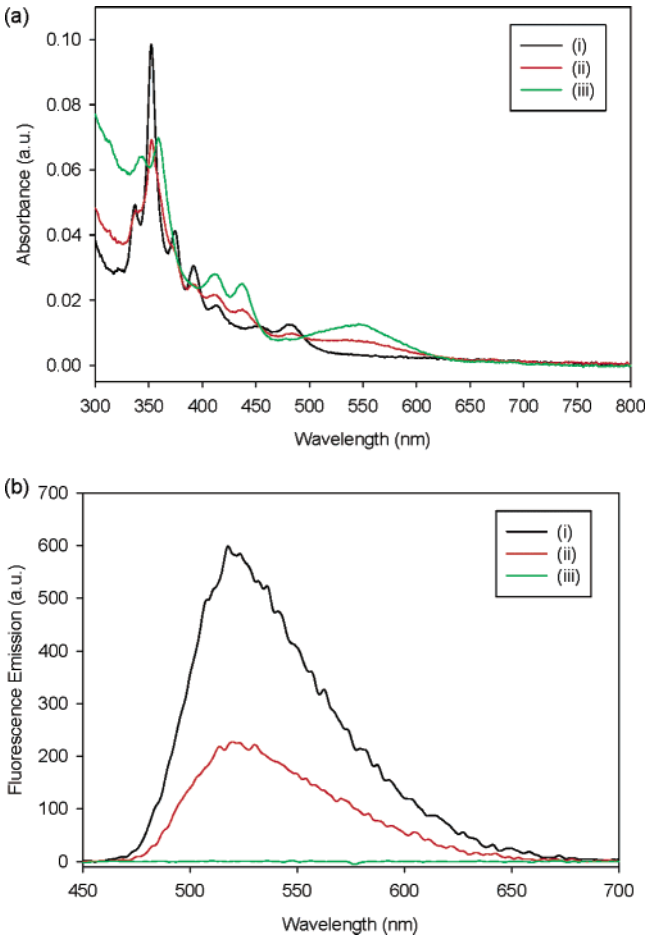

Figure 1. The (a) absorption and (b) emission spectra of **1** in THF (4 mL, 6.7×10^{-7} M) on addition of (i) 0 μL, (ii) 20 μL, and (iii) 180 μL of $[Pd(\eta^3\text{-}C_3H_5)(CH_3CN)_2]^+$ (4.37×10^{-4} M).

on the distribution of π-electrons throughout the ligand framework and is particularly marked in the low-energy region of the UV−vis spectrum where the bands move almost 60 nm to longer wavelength. The band at 376 nm disappears on complexation, and the band at 355 nm decreases in intensity. This suggests that both absorptions have n−π* character in **1**.[16] Recording the UV−vis spectra of **2** in solvents of increased polarity results in a red-shift in the metal perturbed LC (ligand-centered) bands throughout the 340−700 nm spectral region.

While the heterosuperbenzene ligand has an intense emission with $\lambda_{max} = 523$ nm in THF, upon coordination to Pd(II) this emission is efficiently quenched. The changes in the UV−vis and fluorescence spectra on coordination mimic the behavior seen on addition of trifluoroacetic acid to **1**.[1] This implies that none of the absorption bands seen in **2** are metal-based and that an efficient radiationless decay process similar to that which occurs on protonation of **1** is causing the quenching of the emission in **2**.

Synthesis and Characterization of 3a, 3b, and 5. The ruthenium complex $[Ru(bpy)_2(\mathbf{1})]^{2+}$ **3a** and its deuterated analogue $[Ru(d_8\text{-}bpy)_2(\mathbf{1})]^{2+}$ **3b** were prepared by direct reaction of *cis*-$[Ru(bpy)_2Cl_2]$ or *cis*-$[Ru(d_8\text{-}bpy)_2Cl_2]$ with **1** (Scheme 1). Complexation was facilitated by the use of a high

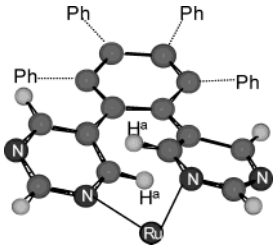

Figure 2. ChemDraw representation showing the steric hindrance between H^a protons of the coordinated polyphenylene in **5**.

boiling solvent (diethylene glycol ethyl ether).[17] Attempts to prepare complex **5** by reacting **4**[1] with $[Ru(bpy)_2Cl_2]$ or $[Ru(bpy)_2(MeCN)_2]^{2+}$ were unsuccessful; however, reaction with $[Ru(bpy)_2(CH_3COCH_3)_2]^{2+}$ in refluxing *n*-BuOH gave **5** in good yield. The reduced reactivity of **4** as compared to that of **1** may be attributed to steric hindrance.

3a and **3b** were characterized by ^{1}H NMR spectroscopy, ESI-MS, and accurate mass spectrometry. The ESI-mass spectrum of the intensely green **3a** showed a single isotopic envelope at *m*/*z* 581.6, assigned to $[M - 2PF_6]^{2+}$ with peaks in the envelope at $^1/_2$ mu intervals. Analogous signals were observed for **5**, along with the ligand labilization product $[Ru(bpy)_2(MeCN)_2]^{2+}$. As for **2**, elemental analyses of **3a** and **3b** could not be obtained, due to incomplete combustion.[14] Accurate mass analyses were obtained instead for **3a** and **5** in acetonitrile and were in accord with calculated values.

The thermal and photochemical stability of **3a** is in marked contrast to that of **5**. The instability in **5** is due to the steric strain imposed by the H^a protons of the polyphenylene. These protons are forced into close proximity in **5** but are absent in **3a** due to cyclodehydrogenation (see Figure 2). Spectroscopic and mass spectral evidence show that **5** decomposes rapidly on irradiation with visible light via loss of the polyphenylene ligand.[15] In essence, this photolability is the result of the weak-field σ-donor character of the coordinated polyphenylene ligand as compared to bpy ligand which allows population of the photochemically active ^{3}MC excited state by reducing the ^{3}MC to ^{3}MLCT energy gap.[5e,g,18]

In the ^{1}H NMR spectra of **3a** and **3b**, two aliphatic signals are observed at δ 1.89 (18H) and δ 1.80 (18H), assigned to the *tert*-butyl protons, and five aromatic signals (2H each) are observed, for the H1−5 protons of coordinated **1** (see Scheme 1 for atom-labeling scheme). All of the aromatic protons of **1** in complex **3** resonate downfield of those of the free ligand (see Figure 3) apart from the H1 protons, ortho to the two pyrimidine nitrogen atoms. These H1 protons point toward the shielding face of a pyridine ring on an adjacent bpy ligand and, as a result, undergo a 0.6 ppm upfield shift in $CDCl_3$ from δ 9.79 in the free ligand to δ 9.18 in the complexes. Attempts to assign the remaining H2−5, N−HSB proton signals in **3a**/**3b**, using nOe experiments, were unsuccessful. This may be attributable to a fast relaxation mechanism that is interfering with the nuclear Overhauser effect.

The chemical shifts for the aromatic protons of the two bpy ligands of **3a**, which are chemically equivalent, have been

(16) (a) Lytle, F. E.; Hercules, D. M. *J. Am. Chem. Soc.* **1969**, *91*, 253. (b) Wayne, R. P. *Principles and Applications of Photochemistry*; Oxford University Press: New York, 1980.

(17) Baranoff, E.; Collin, J.-P.; Furusho, Y.; Laemmel, A. C.; Sauvage, J.-P. *Chem. Commun.* **2000**, 1935−1936.

(18) (a) Laemmel, A. C.; Collin, J.-P.; Sauvage, J.-P. *Eur. J. Inorg. Chem.* **1999**, 383−386. (b) Fanni, S.; Keyes, T. E.; O'Connor, C. M.; Hughes, H.; Wang, R.; Vos, J. G. *Coord. Chem. Rev.* **2000**, *208*, 77−86.

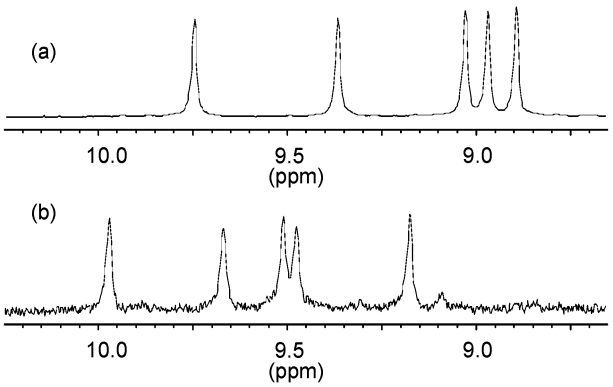

Figure 3. The low-field, aromatic region of the ^{1}H NMR spectra of (a) N−HSB **1** and (b) **3a** ($CDCl_3$, room temperature, 400 MHz).

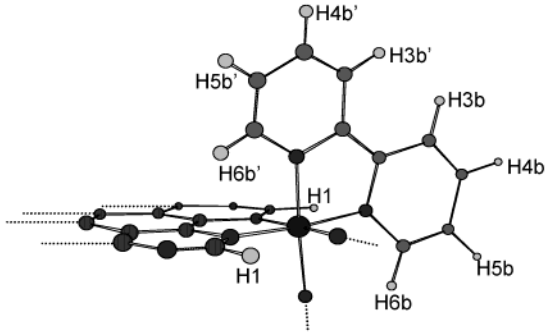

Figure 4. The atom-labeling scheme for the bipyridyl protons of **3a**.

assigned from their coupling patterns, ^{1}H−^{1}H TOCSY spectra, and by comparison with data reported for similar complexes such as $[Ru(bpy)_2(phen)]^{2+}$ (where phen = 1,10-phenanthroline).[19] The four signals at δ 8.58, δ 8.00, δ 7.16, and δ 8.00 in CD_3CN are assigned to the protons H3b′, H4b′, H5b′, and H6b′ respectively. As a result of the influence of the ring current of the large, rigid, aromatic N−HSB, these protons resonate upfield of H3b, H4b, H5b, and H6b (see Figure 4). H6b′ in particular is pushed deep into the shielding conjugated π-system of the adjacent N−HSB, and as a consequence its chemical shift is 0.7 ppm upfield of that observed in free bpy.

The ^{1}H NMR spectra of **3a** show considerable concentration dependence and temperature dependence (see Figure 5). On increasing dilution (3×10^{-3} to 3×10^{-4} M) or temperature (21−60 °C), there is a significant downfield shift of the N−HSB protons H2−5 in **1**. All signals sharpen, but this effect is most marked in the resolution of the coupling of the bpy protons H3b′−6b′ for which broad, featureless signals become resolved doublets and triplets. The addition of benzene to the NMR sample of **3a** similarly sharpens the signals. These changes in chemical shift and resolution are consistent with extensive aggregation forming solution species held together by $\pi-\pi$ stacking interactions between coordinated N−HSB ligands (see Figure 6).[10,20] The steric influence of the bpy ligands is thought to direct the formation of discrete dimers rather than higher aggregates.[20c,d] The introduction of a competing stacking molecule such as benzene then perturbs this aggregation. At low concentrations ($<3 \times 10^{-4}$ M), it may be that the presence

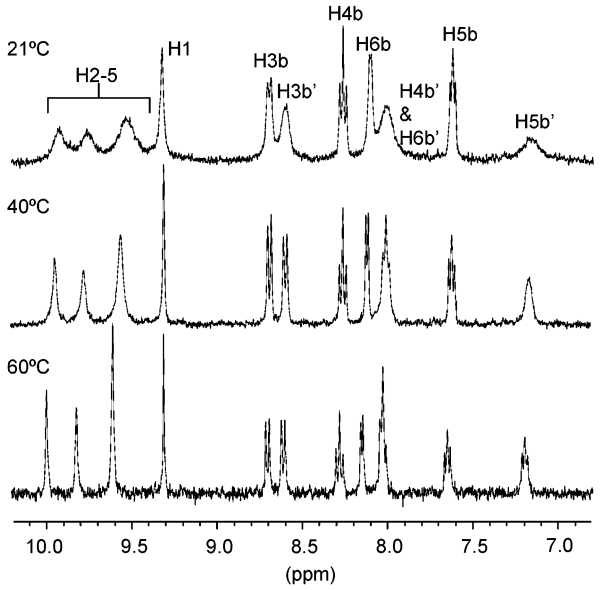

Figure 5. The aromatic region of the ^{1}H NMR spectrum of **3a** at 21, 40, and 60 °C (CD_3CN, 400 MHz).

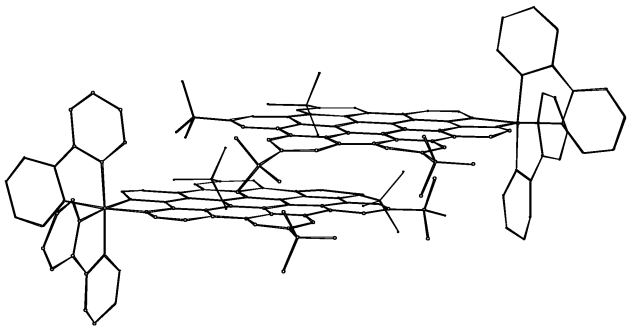

Figure 6. Pictorial model to illustrate the proposed aggregation of **3a** and **3b**.

of *tert*-butyl groups on **1** hampers even the dimeric aggregation proposed. Further investigation into the aggregation of **3a** is ongoing because this type of supramolecular behavior is an important consideration in future optoelectronic applications.

Electrochemical Properties of 3a. Cyclic voltammograms of **3a** in acetonitrile have the features characteristic of Ru(II) polypyridine complexes: a metal-centered (Ru^{II}/Ru^{III}) redox process at anodic potentials and a series of waves at cathodic potentials, corresponding to quasi-reversible one-electron processes of the ligands.[5a,e] The redox potentials in **3a** have been correspondingly assigned (see Table 1).

In similar Ru(II) complexes such as $[Ru(bpy)_2(phen)]^{2+}$ [21] and $[Ru(bpy)_2(dppz)]^{2+}$ (where dppz = dipyrido[3,2-a:2′,3′-c]-phenazine),[6,22] one-electron reduction processes occur on each ligand consecutively. In **3a**, we see two sequential one-electron

(19) (a) Ye, B. H.; Chen, X. M.; Zeng, T. X.; Ji, L. N. *Inorg. Chim. Acta* **1995**, *240*, 5−11. (b) Hua, X.; von Zelewsky, A. *Inorg. Chem.* **1995**, *34*, 5791−5797. (c) Wu, F.; Riesgo, E.; Pavalova, A.; Kipp, R. A.; Schmehl, R. H.; Thummel, R. P. *Inorg. Chem.* **1999**, *38*, 5620−5628.

(20) (a) Shetty, A. S.; Zhang, J.; Moore, J. S. *J. Am. Chem. Soc*. **1996**, *118*, 1019−1027. (b) Bilakhiya, A. K.; Tyagi, B.; Paul, P.; Natarajan, P. *Inorg. Chem*. **2002**, *41*, 3830−3842. (c) Gut, D.; Rudi, A.; Kopilov, J.; Goldberg, I.; Kol, M. *J. Am. Chem. Soc*. **2002**, *124*, 5449−5456. (d) Ishow, E.; Gourdon, A.; Launay, J.-P. *Chem. Commun*. **1998**, 1909−1910. (e) Rudi, A.; Kashman, Y.; Gut, D.; Lellouche, F.; Kol, M. *Chem. Commun.* **1997**, 17−18. (f) Bolger, J.; Gourdon, A.; Ishow, E.; Launay, J.-P. *Inorg. Chem.* **1996**, *35*, 2937−2944. (g) Bolger, J.; Gourdon, A.; Ishow, E.; Launay, J.-P. *J. Chem. Soc., Chem. Commun.* **1995**, 1799−1800. (h) Fechtenkötter, A.; Tchebotareva, N.; Watson, M. D.; Müllen, K. *Tetrahedron* **2001**, *57*, 3769−3783.

(21) Caspar, J. V.; Meyer, T. J. *Inorg. Chem.* **1983**, *22*, 2444−2453.

(22) Amouyal, E.; Homsi, A.; Chambron, J.-C.; Sauvage, J.-P. *J. Chem. Soc., Dalton Trans.* **1990**, *6*, 1841−1845.

Table 1. Electrochemical Data for **3a**, $[Ru(bpy)_3]^{2+}$, and $[Ru(bpy)_2(eilatin)]^{2+}$ in Acetonitrile[a]

	redox potentials (V vs SCE) (ΔEp (mV))				
complex	Ru(II)/Ru(III)	ligand reduction processes			
3a	+1.35 (110)	−0.54 (130)	−1.01 (90)	−1.59 (110)	−1.83 (150)
$[Ru(bpy)_2(eilatin)]^{2+}$ [10c]	1.38 (70)	−0.40 (60) −0.59 (60)	−0.99 (60)	−1.54 (60)	−1.78
$[Ru(bpy)_3]^{2+}$ [5e]	+1.27 (80)	−1.35 (50)		−1.54 (80)	−1.79 (80)

[a] Redox potentials are given in acetonitrile versus SCE, with 0.1 M Bu_4NPF_6 as supporting electrolyte.

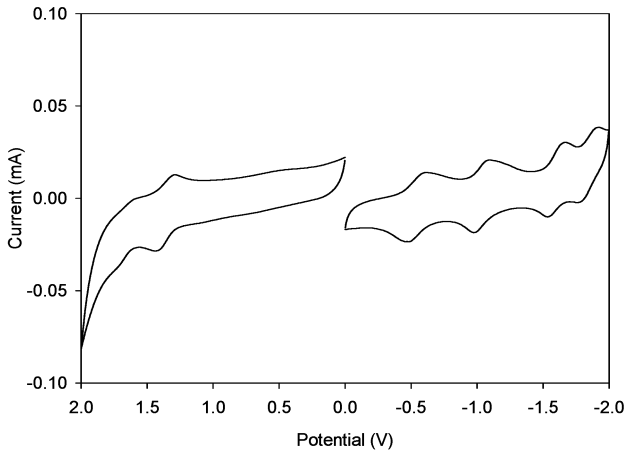

Figure 7. Cyclic voltammograms of **3a** in acetonitrile versus SCE, with 0.1 M Bu_4NPF_6 as supporting electrolyte (scan rate = 500 mV s^{-1}).

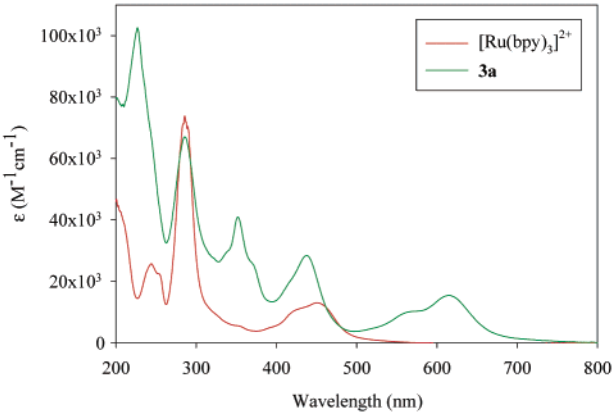

Figure 8. The absorption spectra of **3a** and $[Ru(bpy)_3]^{2+}$ in acetonitrile solution.

reductions for coordinated **1** at −0.54 and −1.01 V (vs SCE), which are significantly anodically shifted with respect to those of the bpy-based reductions, −1.59 and −1.83 V (vs SCE) (see Figure 7). This predictable although uncommon behavior occurs because the lowest π^*-orbital of **1** is much lower in energy than the lowest π^*-orbital of the bpys. This is a direct result of the extensive delocalization in **1**. As expected, these N−HSB reduction processes occur more readily in the complex than in the free ligand where they are observed at −1.20 and −1.64 V (vs SCE) in chloroform.[15]

No oxidation process was observed in the free ligand N−HSB within the potential window investigated. However, **3a** undergoes two observable oxidation processes. The more distinct at +1.35 V (vs SCE) is assigned to the metal-centered (Ru^{II}/Ru^{III}) process. This occurs at more positive potential than that of $[Ru(bpy)_3]^{2+}$ (see Table 1), indicating that the π-acceptor properties of **1** make electron abstraction from the metal center more difficult.[5a,e]

Electronic Absorption of 3a. Analogous to other polypyridyl ruthenium complexes,[5e] the ultraviolet region of the absorption spectrum of **3a** (see Figure 8) is dominated by the ligand-centered (LC) $\pi \rightarrow \pi^*$ transitions on bpy (286 nm) and **1** (227 and 352 nm). The visible region of the spectrum is characterized by the presence of two bands that can be attributed to two separate ^{1}MLCT transitions (437 and 615 nm). In combination, these are responsible for the strong green color of the complex.[8,23] The intense band centered at 437 nm is the ^{1}MLCT transition to coordinated bpy (see Table 2, cf. $[Ru(bpy)_3]^{2+}$, 450 nm). The red-shifted absorption band centered at 615 nm, which is not present in the free ligand spectrum, is due to a ^{1}MLCT transition to the N−HSB ligand. The unusually low energy of this transition is indicative of the presence of very low-lying π^*-acceptor orbitals in the highly delocalized N−HSB. The presence of two ^{1}MLCT bands in the absorption spectrum of **3**, one for each type of ligand, is also observed in other Ru(II) mixed ligand complexes such as $[Ru(bpy)_2(bpz)]^{2+}$,[5e] $[Ru(bpy)_2(biq)]^{2+}$,[5e] $[Ru(bpy)_2(dppz)]^{2+}$,[6] and $[Ru(bpy)_2(eilatin)]^{2+}$ [20e] (bpz = 2,2′-bipyrazine and biq = 2,2′-biquinoline).

Spectroelectrochemistry of 3a. The oxidation of complex **3a** at a potential just above that of the Ru(II/III) redox process (+1.4 V) was followed by UV−vis spectroscopy (see Figure 9). The generation of the oxidized species is identified by a decrease in the intensity of the ^{1}MLCT bands at around 416 and 615 nm and the formation of new weak bands at around 400, 500, and 850 nm. The spectra show clear isobestic points at 379, 408, 463, 545, and 665 nm, indicating that a single oxidation process is occurring. While the processes were reversible in acetonitrile, the oxidized product was unstable in dichloromethane over extended periods.

As can be seen in Figure 9, a moderately intense band in the near-IR at 850 nm is observed for the oxidized form of **3a**. By comparison to related complexes, this new weak band is assigned as a ligand-to-metal charge-transfer (LMCT) band involving N−HSB **1**.[24] The energy and the intensity of LMCT transitions have been correlated to the electron density and σ-donor character of the ligands, with more intense bands being observed when electron-rich ligands are employed.

Electronic Emission of 3a. Following electronic excitation of Ru(II)−polypyridyl complexes, rapid relaxation occurs to form an emissive ^{3}MLCT state in which the electron is localized on the ligand having the lowest-energy π^*-acceptor orbital.[8,25] Irradiation within the ^{1}MLCT absorption band of **3a** at 615 nm

(23) (a) Seddon, E. A.; Seddon, K. R. *The Chemistry of Ruthenium*; Elsevier: New York, 1984; Chapter 15. (b) Thummel, R.; Lefoulon, F.; Korp, J. D. *Inorg. Chem.* **1987**, *26*, 2370−2376.

(24) (a) Nazeeruddin, M. K.; Zakeeruddin, S. M.; Kalyanasundaram, K. *J. Phys. Chem.* **1993**, *97*, 9607. (b) Kalyanasundaram, K.; Zakeeruddin, S. M.; Nazeeruddin, Md. K. *Coord. Chem. Rev.* **1994**, *132*, 259−264

(25) Danzer, G. D.; Golus, J. A.; Kincaid, J. R. *J. Am. Chem. Soc.* **1993**, *115*, 8643−8648.

Table 2. UV−Vis Spectral Data for **3a** and $[Ru(bpy)_3]^{2+}$ in Acetonitrile at Room Temperature

complex	wavelength (nm) (ϵ (M^{-1} cm^{-1}))					
3a	227 (103×10^3)		286 (67×10^3)	352 (41×10^3)	437 (28×10^3)	615 (15×10^3)
$[Ru(bpy)_3]^{2+}$		240 (25×10^3)	285 (74×10^3)		450 (13×10^3)	

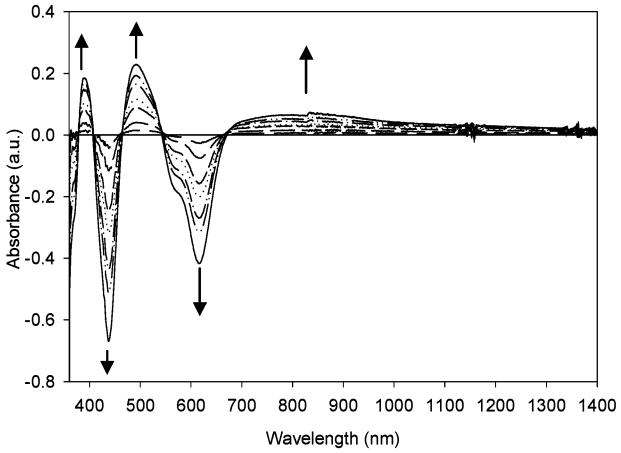

Figure 9. Visible and near-IR "differential" spectra of **3a** in dichloromethane with 0.1 M Bu_4NPF_6 at +1.4 V. The arrows indicate the changes over time.

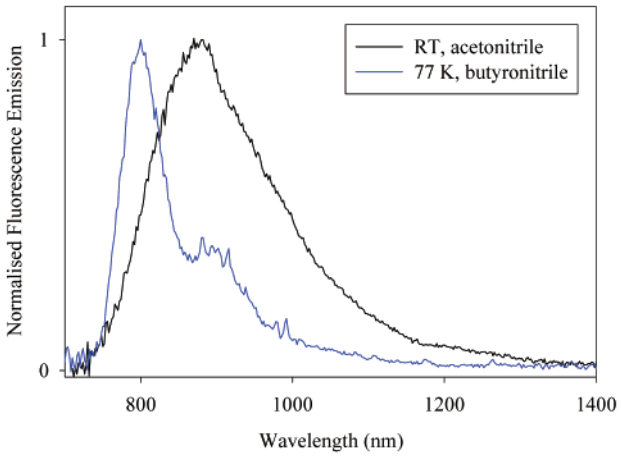

Figure 10. The corrected emission spectra of **3a** after irradiation at 615 nm at room temperature and 77 K.

results in the observation of a broad, near-infrared luminescence with λ_{max} at 880 nm and a lifetime of 13 ns (±1 ns) in acetonitrile (see Figure 10). Comparison of the energy (λ_{max}^{em}) and excited-state lifetime of the luminescence with those of related ruthenium mixed polypyridine complexes suggests that the ^{3}MLCT emission is t_{2g}-to-π^*(**1**)-based.[5g] The luminescence is considerably red-shifted because of the lower energy of the ^{3}MLCT state as compared to that of $[Ru(bpy)_3]^{2+}$ and has a shorter lifetime than that of $[Ru(bpy)_3]^{2+}$ (see Table 3). These effects are due to the much reduced ground-state to excited-state energy gap (cf. energy gap law).[21,26] **3a** is emissive in all of the solvents investigated; however, the energy (λ_{max}^{em}), the lifetime (τ), and the emission quantum yield (Φ_{em}) are strongly solvent-dependent. As expected, in low-temperature rigid glasses, the emission is blue-shifted, and the emission lifetime increases. The emission spectrum of **3a** in butyronitrile at 77 K on irradiation at 615 nm (see Figure 10) displays a structured

(26) Caspar, J. V.; Meyer, T. J. *J. Am. Chem. Soc.* **1983**, *105*, 5583−5590.

Table 3. Spectroscopic Properties of the Near-Infrared Emitter **3a** in Various Deaerated Solvents Together with Those of $[Ru(bpy)_3]^{2+}$ at Room Temperature

complex	solvent	λ_{max}^{abs} (nm) (ϵ (M^{-1} cm^{-1}))	λ_{max}^{em} (nm)	τ (ns)	ϕ_{em}
3a	$CHCl_3$	620 (8×10^3)	840	39	7×10^{-4}
3a	CH_3CN	615 (15×10^3)	880	13	4×10^{-4}
3a	methanol:ethanol[b]		790[b]	320[b]	
3a	butyronitrile[b]		800[b]		
$[Ru(bpy)_3]^{2+}$[a]	CH_3CN	452 (13×10^3)	615	800	6.2×10^{-2}

[a] Reference 28. [b] 77 K.

band with a λ_{max}^{em} centered at 800 nm. This emission shows vibrational structure[27] and has a monoexponential lifetime. The results are summarized along with the excited-state lifetimes and emission quantum yields in Table 3.

When exciting **3a** with λ < 500 nm, in addition to an emission band at 880 nm, a band with the same shape and lifetime as that of **1** is observed. By comparison with the photophysical properties of **1**,[1] this additional emission (λ = 550 nm, τ = 10.6 ns) can be attributed to trace amounts (<0.1%) of free N−HSB.

In theory, the ^{3}MLCT state in **3**a is localized either on the bpy, on the N−HSB (**1**), or on a component of a ligand.[18b] To investigate this further, the excited-state lifetime of the deuterated analogue **3b** was measured. Deuteriation of ligands not involved directly in the emission process should not influence the emission quantum yield or lifetime.[29] In our case, **3b** exhibits the same emission lifetime (370 ns ± 10%, 77 K) as **3a**, indicating that the bpys are spectator ligands and the emission is indeed N−HSB-based.

Preliminary studies indicate that, within the experimental conditions outlined, the spectroscopic properties of **3a** are essentially independent of the degree of protonation of the uncoordinated imine nitrogens in the complex. Addition of up to 40 equiv of trifluoromethanesulfonic acid to a 1.4×10^{-4} M chloroform solution of **3a** results in no variation in the absorption and emission spectra. This is in contrast to the pH-dependent spectroscopic behavior of **1**. On coordination, the free imine nitrogens experience a decrease in electron density and are consequently less basic. Further studies of the electronic properties of **3a** as a function of protonation are underway to provide more information about the pK_a of the excited state of **3a**.

Conclusion

The nitrogen heterosuperbenzene, N−HSB **1**, has proven to be a remarkable and versatile ligand in two new Pd(II) and Ru(II) complexes. The former is an interesting model candidate for Pd dispersed graphite, and the catalytic properties of this

(27) Di Donato, E.; Tommasini, M.; Fustella, G.; Brambilla, L.; Castiglioni, C.; Zerbi, G.; Simpson, C. D.; Müllen, K.; Negri, F. *Chem. Phys.* **2004**, *301*, 81−93.
(28) Barigelletti, F.; De Cola, L.; Balzani, V.; Belser, P.; von Zelewsky, A.; Vögtle, F.; Ebmeyer, F.; Grammenudi, S. *J. Am. Chem. Soc.* **1989**, *111*, 4662−4668.
(29) Browne, W. R.; Vos, J. G. *Coord. Chem. Rev.* **2001**, *219*−*221*, 761−787.

compound are under investigation. The latter heteroleptic Ru(II) polyimine is a near-IR emitter and a black MLCT absorber. The N−HSB ligand combines a number of desirable features that enhance the photophysical properties of the $[Ru(bpy)_2]^{2+}$ center to which it is coordinated. It possesses the exceptionally low-lying π^*-acceptor orbitals necessary to red-shift the MLCT and an unprecedented degree of delocalization and rigidity. The latter normally assists in decreasing nonradiative decay. Preliminary work on stepwise modifications to N−HSB and the generation of the resulting homo- and heteroleptic complexes is underway, but there is no doubt that $[Ru(bpy)_2(\mathbf{1})]^{2+}$ represents a step forward in the design of a chemically accessible and tuneable photoactive material. We anticipate that **3a** could potentially find use in solid-state electroluminescent devices. Recent research in this area has demonstrated that polymer-embedded Ru(II) polypyridyl complexes show fully reversible voltage-dependent color-switching.[30,31] It would seem that the unique electron-accepting and delocalized nature of the ligands are key to the color-switching phenomenon.[31]

Experimental Section

$RuCl_3 \cdot H_2O$, $PdCl_2$ (Johnson-Matthey), 2,2′-bipyridine (bpy) (Aldrich), d_8-2,2′-bipyridine (d_8-bpy) (Complex Solutions (Dublin)), and allyl chloride (BDH Ltd.) were used as received. $[Ru(bpy)_2Cl_2]\cdot 2H_2O$,[32] $[Ru(bpy)_3](PF_6)_2$,[26] $[Ru(bpy)_2(CH_3COCH_3)_2]^{2+}$,[32] bis(chloro-$\eta^3$-allyl palladium),[13] and **1**[1] were synthesized according to literature procedures. All reactions were carried out under an argon atmosphere using standard Schlenk techniques. Flash chromatography was performed using silica gel (Brockman I, Aldrich Chemical) as the stationary phase.

Synthesis. [Pd(η^3-C_3H_5)(1)](PF$_6$) (2). Bis(chloro-η^3-allyl palladium) (4.9 mg; 1.33×10^{-2} mmol) was dissolved in acetonitrile (2 mL) with five drops of dichloromethane. $AgNO_3$ (7 mg; 4.1×10^{-2} mmol) was added, and the solution was stirred at ambient temperature for 6 h. AgCl was removed by filtration over Celite. Compound **1** (20 mg; 2.66×10^{-2} mmol) in toluene (5 mL) was added dropwise to the filtrate, and the reaction mixture was stirred for 12 h. The red precipitate was collected and taken up in a minimum of acetonitrile, and a saturated NH_4PF_6 aqueous solution was added, to form a dark red solid, which was separated by filtration. Yield: 20 mg, 84%. ^{1}H NMR ($CDCl_3$): δ 9.45, 9.40, 9.34, 9.18 (s, 2H, H_{aryl}), 8.56 (s, 2H, H1), 5.61 (s, 1H, H^{meso}), 4.24 (s, 2H, H^{syn}), 2.87 (s, 2H, H^{anti}), 1.96, 1.86 (s, 18H, $-CH_3$). ESI-MS (CH_3OH) *m*/*z* (%) $[M - PF_6]^+$ 898.1 (100) (calcd 898.4). ESI-MS (CH_3OH); calcd for $C_{57}H_{51}N_4Pd$, $[M - PF_6]^+$ *m*/*z* 897.3148; found, 897.3182. IR (KBr disk, cm^{-1}): 2960s, 2930s, 2868s, 1605m, 1535m, 1465m, 1398s, 1380s, 1249m, 1065w, 1025m, 842vs, 558s.

[Ru(bpy)$_2$(1)](PF$_6$)$_2$ (3a). Compound **1** (20 mg; 2.66×10^{-2} mmol) and $[Ru(bpy)_2Cl_2]\cdot 2H_2O$ (15.4 mg; 2.96×10^{-2} mmol) were sonicated in diethylene glycol ethyl ether (5 mL) for 10 min. The brown solution was degassed by passing a stream of argon through the solution for 30 min. After the solution was heated for 20 h at 127 °C under an argon atmosphere, it was allowed to cool to room temperature and was filtered. To the mixture was added a saturated NH_4PF_6 aqueous solution to form a dark green solid, which was separated by filtration and washed with water and diethyl ether. Chromatography (SiO_2, 100:10:1 acetonitrile:water:KNO_3 (aq)) followed by anion exchange gave $[Ru(bpy)_2(\mathbf{1})](PF_6)_2$ as a black-green solid. Yield: 0.023 mg, 60%. ^{1}H NMR (CD_3CN): δ 9.94 (s, 2H, H_{aryl}), 9.80 (s, 2H, H_{aryl}), 9.60 (s, 4H, H_{aryl}), 9.31 (s, 2H, H1), 8.67 (d, 2H, $^3J_{HH} = 8.2$, H3b), 8.58 (br d, 2H, $^3J_{HH} = 7.5$, H3b′), 8.25 (t, 2H, $^3J_{HH} = 8.2$, H4b), 8.10 (d, 2H, $^3J_{HH} = 5.5$, H6b), 8.00 (m, 4H, H4b′, H6b′), 7.63 (t, 2H, $^3J_{HH} = 6.0-7.5$, H5b), 7.17 (br s, 2H, H5b′), 1.88, 1.83 (s, 18H, $-CH_3$). ESI-MS (CH_3CN) *m*/*z* (%) $[M - 2PF_6]^{2+}$ 581.6 (100) (calcd 582.2). ESI-MS (CH_3CN); calcd for $C_{74}H_{62}N_8Ru$, $[M - 2PF_6]^{2+}$ *m*/*z* 582.2071; found, 582.2042. IR (KBr disk, cm^{-1}): 2958s, 2927s, 2867m, 1719m, 1605m, 1466m, 1381s, 1257m, 1171m, 1120m, 1072m, 848vs, 767m, 557s.

[Ru(d_8-bpy)$_2$(1)](PF$_6$)$_2$ (3b). This was synthesized the same as for **3a**, except **1** (20 mg; 2.66×10^{-2} mmol) and $[Ru(d_8\text{-bpy})_2Cl_2]\cdot 2H_2O$ (16 mg; 3.20×10^{-2} mmol) were used, yielding $[Ru(d_8\text{-bpy})_2(\mathbf{1})](PF_6)_2$ (**3b**) as a black-green solid. Yield: 0.018 mg, 90%. ^{1}H NMR (CD_3CN): δ 9.90 (s, 2H, H_{aryl}), 9.71 (s, 2H, H_{aryl}), 9.42 (s, 4H, H_{aryl}), 9.31 (s, 2H, H1), 1.84 (br s, 36H, $-CH_3$). ESI-MS (CH_3CN) *m*/*z* (%) $[M - 2PF_6]^{2+}$ 590.3 (100) (calcd 590.2). IR (KBr disk, cm^{-1}): 2958s, 2910m, 2868m, 1606m, 1560m, 1458m, 1382s, 1337m, 1247m, 1173w, 1088w, 1005w, 848vs, 585w, 557s.

[Ru(bpy)$_2$(4)](PF$_6$)$_2$ (5). A mixture of $[Ru(bpy)_2Cl_2]\cdot 2H_2O$ (15.0 mg; 2.88×10^{-2} mmol) and $AgBF_4$ (13.0 mg; 6.54×10^{-2} mmol) was heated at reflux in acetone (20 mL) for 1.5 h. The silver chloride formed was separated by filtration and washed with acetone. *n*-BuOH (20 mL) was added, and the acetone evaporated. **4** (20 mg; 2.62×10^{-2} mmol) was dissolved in dichloromethane (5 mL), *n*-BuOH (10 mL) was added, and the dichloromethane evaporated. This solution was added to the reaction mixture and was refluxed for 72 h under an argon atmosphere. After being cooled to room temperature and filtration, the solvent was removed in vacuo. The minimum amount of acetonitrile was added to dissolve the solid, and a saturated NH_4PF_6 aqueous solution was added to the mixture to form a red-brown solid, which was separated by filtration and washed with water and diethyl ether. Chromatographic purification and spectroscopic analysis of this compound was prevented by the rapid decomplexation of **4** in solution.[15] Estimated yield based on ESI-MS data: 0.019 mg, 55%. ESI-MS (CH_3CN) *m*/*z* (%) $[M - 2PF_6]^{2+}$ 588.2 (100) (calcd 588.2). ESI-MS (CH_3CN); calcd for $C_{74}H_{74}N_8Ru$, $[M - 2PF_6]^{2+}$ *m*/*z* 588.2540; found, 588.2537.

Physical Measurements and Instrumentation. IR spectra were recorded from KBr disks on a Perkin-Elmer Paragon 1000 Fourier transform spectrophotometer. NMR spectra were recorded on DPX 400 spectrometer operating at 400.13 MHz for ^{1}H, and 100.62 MHz for ^{13}C, and were standardized with respect to TMS. Electrospray mass spectra were recorded on a micromass LCT electrospray mass spectrometer. Accurate mass spectra were referenced against Leucine Enkephalin (555.6 g mol^{-1}) and were reported within 5 ppm.

UV−vis absorption spectra were recorded on a Shimadzu UV-2401PC, UV−vis recording spectrophotometer. The emission spectra for **2** were not corrected and were recorded at 25 °C using an Edinburgh Instrument, equipped with an E-Germanium ($\lambda_{em} = 610$ nm Emission filter: cut off 780 nm). The NIR luminescence spectra for **3** were obtained with an Edinburgh FLS920 spectrometer equipped with a Hamamatsu R5509-72 supercooled photomultiplier tube (193 K) and a TM300 emission monochromator with NIR grating blazed at 1000 nm; a 450 W xenon arc lamp was used as the light source. The emission spectra were corrected to compensate for the photomultiplier response in the different spectral regions. Quartz cells (10 mm path length) were used. Emission quantum yields were measured at room temperature in deaerated solutions using $[Ru(bpy)_3]^{2+}$ ($\Phi_F = 0.028$, room temperature, water, air equilibrated solution)[33] as the quantum yield standard. Luminescence lifetime measurements were obtained using an Edinburgh Analytical Instruments (EAI) time-correlated single-photon counting apparatus (TCSPC) composed of two model J-yA monochromators (emission and excitation), a single-photon photomultiplier detection system model 5300, and a F900 nanosecond flashlamp (N_2 filled at 1.1 atm pressure, 40 kHz), interfaced with a personal computer via a Norland MCA card. A 500 nm cutoff filter was used in emission to attenuate scatter of the excitation light (337 nm). Data correlation and

(30) Slinker, J.; Bernards, D.; Houston, P. L.; Abruña, H. D.; Bernhard, S.; Malliaras, G. G. *Chem. Commun.* **2003**, 2392−2399.
(31) Welter, S.; Brunner, K.; Hofstraat, J. W.; De Cola, L. *Nature* **2003**, *421*, 54−57.
(32) Sullivan, B. P.; Salmon, D. J.; Meyer, T. J. *Inorg. Chem.* **1978**, *17*, 3334−3341.
(33) Nakamaru, K. *Bull. Chem. Soc. Jpn.* **1982**, *55*, 2697.

manipulation were carried out using EAI F900 software version 5.1.3. Samples were deaerated for 20 min using Ar gas before measurements were carried out. Emission lifetimes were calculated using a single-exponential fitting function; a Levenberg−Marquardt algorithm with iterative reconvolution Edinburgh instruments F900 software was used; uncertainty is 10%. The reduced χ^2 and residual plots were used to judge the quality of the fits.

Electrochemical measurements were carried out on a model 660 electrochemical workstation (CH Instruments). Typical concentrations were $0.2-1.0 \times 10^{-4}$ M in anhydrous solutions containing 0.1 M tetrabutylammonium hexafluorophosphate (Bu_4NPF_6). Conventional voltammetric measurements were carried out using a standard three-electrode cell arrangement. A Teflon shrouded glassy carbon working electrode, a Pt wire auxiliary electrode, and an SCE reference electrode were employed. Solutions were deoxygenated by purging with N_2 gas for 15 min prior to the measurement. Measurements were made in the range −2.0 to +2.0 versus SCE.

Spectroelectrochemistry was carried out using an OTTLE setup composed of a homemade Pyrex glass, thin layer cell (2 mm). The optically transparent working electrode was made from platinum−rhodium gauze, a platinum wire counter electrode, and the reference electrode, which was a pseudo-Ag/AgCl reference electrode. The working electrode was held at the required potential throughout the measurement using an EG&G PAR model 362 potentiostat. UV−vis absorption spectra were recorded on a Shimadzu UV−vis−NIR 3100 spectrophotometer interfaced with an Elonex PC466 using UV−vis data manager.

Acknowledgment. We thank Prof. Maria Teresa Gandolfi, Dr. Roberto Ballardini, and Prof. Ed Constable for useful discussions and Dr. John O'Brien for technical assistance. D.J.G. thanks Enterprise Ireland award IF-2001\369 for financial support.

Supporting Information Available: Variable-temperature ^{1}H NMR spectra of **2**. ESI-mass spectra of **2**, **3a**, and **3b**. ESI-mass spectrum of $[Ru(bpy)_2(\mathbf{4})]^{2+}$, **5**, before and after photolysis. ^{1}H−^{1}H TOCSY NMR spectra of **3a**. Cyclic voltammogram of **1**. This material is available free of charge via the Internet at http://pubs.acs.org.

JA0491634